Effect of Pressure on Vertically Aligned ZnO Nanorods for Piezoelectric Nanogenerator Application

Ashutosh Kumar[1,a], Satya Prakash Singh[1,b], and Vinay Pratap Singh[2,c]

[1] *Department of Physics, Christ Church College Kanpur, Kanpur, Uttar Pradesh, India- 208001.*
[2] *Department of Applied Sciences and Humanities, United College of Engineering and Research, Prayagraj, India- 211010*

[a] ashutoshais@gmail.com
[b] satya1209prakash@gmail.com
[c] vinay.phy@gmail.com

Abstract

The piezoelectric characteristics of zinc oxide (ZnO) nanorods and their prospective uses in energy harvesting, sensing, and nanogenerators have pave off a lot of interest recently. In present work, highly vertically aligned ZnO nanorods grown over Si substrates by hydrothermal method. ZnO nanorods were grown in a two-step process. First an optimum ZnO seed layer developed on a n-type Si wafer by sol-gel method, with particle size of diameter ~ 40 nm as a nucleation site. Subsequently nanorods grown on those sites with the range of length between 250 to 400 nm. These nanorods were examined by FESEM and phase was confirmed with XRD. Study of pressure effect in a Teflon-lined stainless-steel autoclave was performed at 5 bar pressure.

Keywords: Sol-gel, Spin Coating, Vertically Aligned ZnO nanorod, Piezoelectric.
Received 27 January 2025; First Review 23 February 2025; Accepted 23 February 2025

*** Address of correspondence**
Dr. Satya Prakash Singh
Department of Physics, Christ Church College Kanpur, Kanpur, Uttar Pradesh, India- 208001.

Email: satya1209prakash@gmail.com

How to cite this article
Ashutosh Kumar, Satya Prakash Singh, and Vinay Pratap Singh, Effect of Pressure on Vertically Aligned ZnO Nanorods for Piezoelectric Nanogenerator Application, J. Cond. Matt. 2024; 02 (02): 99-103.

Available from:
https://doi.org/10.61343/jcm.v2i02.64

Introduction

A lot of emphasis during the past few years has been seen in the development of nanostructured metal oxides-based chemical, biological and thermo-mechanical sensors. Recently, ZnO nanorods have attracted a lot of attention because of their distinctive qualities and broad range of applications [1]. One-dimensional nanostructures in nanotechnology are notable for their exceptional mechanical, optical, and electrical characteristics, which make them perfect for a range of technological advancements [2]. The high aspect ratio, broad band gap, high surface area, and strong exciton binding energy of ZnO nanorods make them ideal for application in solar cells, light-emitting diodes, photodetectors, photocatalysts, and biosensors [3-7]. ZnO is a readily available, chemically stable, and non-toxic substance that is widely distributed throughout the earth. The extrinsic semiconductor ZnO, also referred to as an n-type semiconductor, has a high exciton-binding energy (60 meV) and a bandgap of about 3.37 eV [8–11]. The preparation of ZnO nanostructures, such as nanowires, nanorods, nanotubes, and nanoflowers, has attracted increasing interest nowadays [12-14]. ZnO can be produced physically using methods such as metal-organic chemical vapour deposition [15], sputtering [16], and molecular beam epitaxy [17]. However, because of the intricate nature of the equipment and the need for high temperatures and low pressures, such processes are costly. Therefore, chemical processes including hydrothermal deposition [18], chemical bath deposition [19], and electrochemical deposition [20] are economical, have the capacity to produce nanoparticles on a large scale, and are very effective for producing them for a variety of application possibilities.

The hydrothermal method has been followed for the growth of vertically aligned nanorods on fluorine doped tin oxide (FTO) coated glass substrates [21] and seedless substrates (Pt/Si, Au/Si, Cu plates, FTO, and ITO coated glass) [22] using zinc nitrate hexahydrate (ZNH) and hexamine as precursors. For the preparation of seed layer on silicon, glass, and FTO coated glass substrates, a sol-gel process using zinc acetate dihydrate (ZAD), ethanol and 2-methoxyethanol was reported [23]. A combination of the two solution processes- seed layer deposition and nanorods growth was reported by Romero et al. [24] who produced nanorods arranged in a flower-like structure on seeded silicon and glass substrates. M. Bakry et al. [25] reported

low-cost fabrication methods of ZnO nanorods and their physical and photoelectrochemical properties for optoelectronic applications. It has been reported that the size (especially the diameter) and shape of the ZnO nanorods greatly affects its properties to be used in applications like photocatalysis [26] and gas sensing [27]. Also, there are several reports on the importance of the seed layer to obtain ZnO nanorods of the desired size, morphology and areal density [28-30].

In this work, the hydrothermal growth of ZnO nanorods on Si/SiO_2 surface has been demonstrated without using any intermediate layer or surface modification. For this, first the ZnO seed layer deposition was optimized using the sol gel method. Then, a hydrothermal method was followed to grow vertically aligned, controlled, reproducible, and scalable zinc oxide nanorods.

Materials and Methods

In this work, the hydrothermal growth of ZnO nanorods on n-type Si surface has been demonstrated without using any intermediate layer or surface modification. For this, first the ZnO seed layer deposition was optimized using the sol gel method. For fabrication of seed layer, we used the precursors, namely, zinc acetate dihydrate (ZAD), isopropanol (IPA) and diethanolamine (DEA). A 0.75 M solution of ZAD in IPA was prepared by stirring at 50 °C for 60 minutes on a magnetic stirrer at 1000 rpm. Equimolar amount of DEA was added to the solution and further stirred for 20 minutes to form a clear and homogeneous solution. Stepped annealing was performed on the sol. for 2 hours to form a yellow-coloured sol to be used for seed layer deposition. The sol was spin coated onto cleaned n-type Si wafer at 4000 rpm for 20 seconds. These substrates were further heated at 400 °C for 15 minutes for hard baking. By this ZnO seed layer with particle size of diameter ~ 40 nm was prepared as a nucleation site.

For the growth of ZnO nanorods, aqueous solution of 2 mM solution of zinc nitrate hexahydrate (ZNH) with equimolar amount of hexamine were prepared in DI water by stirring at 50 °C for 1 hour. Nanorods of ZnO were grown on seed layer deposited substrates by placing the wafer in beakers containing these solutions and heating at 60 °C and 90 °C for 8 hours in an oven.

Characterization

The surface morphology, dimensions of the seed layer films and nanorods were examined by FESEM (TESCAN MIRA3). The X – ray diffraction (XRD) (PAN-analytical Xpert Powder diffractometer with CuKα radiation) analysis was carried out for phase identification.

Results and Discussions

Hydrothermal synthesis is one of the most commonly used methods for preparation of nanomaterials. It is basically a solution reaction-based approach. Hydrothermal synthesis can generate nanomaterials which are not stable at elevated temperatures. Nanomaterials with high vapor pressures can be produced by the hydrothermal method with minimum loss of materials. The compositions of nanomaterials to be synthesized can be well controlled in hydrothermal synthesis through liquid phase or multiphase chemical reactions. It is important to obtain nanoparticles of the desired size and morphology as it affects various properties pertaining to a particular application. The size distribution, homogeneity throughout the entire area, and crystal orientation of the seed layer determine the characteristics of ZnO nanorods developed over it [28, 31]. The dependence of the sensing properties [32] and the photocatalytic properties [33] on the size of the nanoparticles and the microstructural characteristics of the seed layer have also been reported earlier.

During the preparation of sol for the seed layer deposition using IPA as the solvent, the salt ZAD disintegrates to form ions [34]. The complexing agent DEA forms bond with the cation and stabilizes the sol gel. Properties of the solvent, namely, the boiling point and the viscosity of the solvent have been reported to affect the size, homogeneous distribution and preferred orientation of the nanoparticles in the seed layer [35]. The shape and size of the scattered nanoparticles in the sol is depend on diffusion time and the time needed for clusters to form in the sol due to crystallisation [36]. If the diffusion time is less than the time required for cluster formation in the sol, rough aggregates are formed in an oriented manner after crystallization. Therefore, we used a novel two-step liquid phase annealing of the sol to control the size, distribution and morphology of the seed particles in the sol which subsequently resulted in good quality seed layer upon film deposition.

The novel two-step liquid phase annealing accelerated the process of diffusion, enhanced the solubility of the chemical groups in the alcohol which were newly formed as a result of the reaction between ZAD and DEA leading to increased formation of the Zn-O groups throughout the sol. This leads the formation of liquid clusters in an oriented manner. These clusters eventually crystallized as individual nanoparticles after spin coating and baking. It is resulted in an improved morphology of seed layer with discrete nanoparticles of uniform size of ~ 40 nm throughout the substrate, as shown in Figure 1. The n-type substrates were initially heated (soft bake at 250 °C and kept for 10 minutes) and hard baked at 400 °C for 15 minutes immediately after spin coating to remove the solvent, facilitate nucleation, and align the seed crystals.

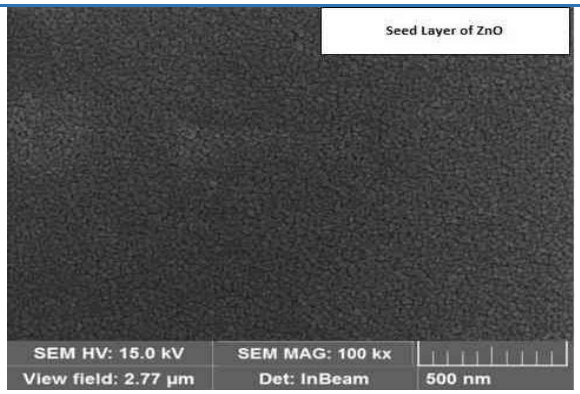

Figure 1: Morphology of ZnO seed layer nanoparticle on Si wafer

The room temperature X-Ray Diffraction (θ – 2θ scan) spectra for the ZnO thin films annealed at temperature of 400 °C is shown in Figure 2. It is evident from Figure 2 that the seed layer of ZnO film shows the polycrystalline behaviour of the film. The intensity of three major peaks corresponding to (0 1 0), (0 0 2) and (0 1 1) Miller planes are clearly observed in XRD pattern. The crystallographic characteristics of the films have been studied using the *'Checkcell'* software and compared with the data of Joint Committee on Powder Diffraction Standards (JCPDS# 79−0206). The XRD data of the annealed thin films fitted well with hexagonal structure of space group $P6_{3mc}$ and calculated lattice parameters are $\boldsymbol{a}$ = 0.3255± 0.0001, $\boldsymbol{b}$ = 0.3255± 0.0001 and $\boldsymbol{c}$ = 0.5217± 0.0001.

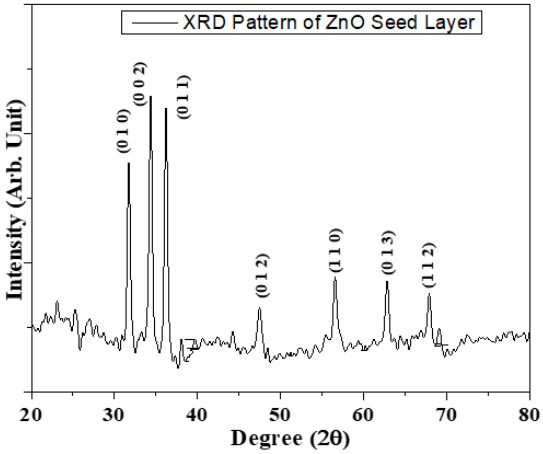

Figure 2: X–ray diffraction pattern of ZnO films.

The diameter and length of nanorods are influenced by the thickness of the seed layer. According to reports, a thinner seed layer encourages the formation of longer nanorods than a thicker one [37]. The seed layer's surface roughness, grain size, and crystal structure all affect how the nanorods align with the substrate [38]. The growth of ZnO nanorods is directly affected by the decomposition of hexamine ($C_6H_{12}N_4$), which was used to grow highly anisotropic nanorods by selectively capping non polar planes of ZnO crystal by the highly water-soluble non-ionic amine derivative. The nanorods were grown over the seeded substrates with varying parameters of temperature and time. The nanorods synthesis was performed at two different temperatures: 60 °C and 90 °C by using concentration of 2mM growth solution for synthesis time 4 hours and 8 hours, under atmospheric pressure. However, formation of nanorods was not observed at growth temperature 60 °C for synthesis times 4 hours and 8hours.

ZnO nanorods with uniform distribution were obtained at 90 °C in all the cases (Figure 3). Cross-sectional FESEM images of these ZnO nanorods for synthesis time of 4 hours and 8 hours are shown in Figure 4 and Figure 5. The dimensions, orientation and the number density of nanorods significantly varied with the precursor concentration and time at the same synthesis temperature. Also, it was observed that, a synthesis time of 4 hours led to the formation of nanorods having a relatively low number density. Nanorods with uniform distribution were obtained at 90 °C in the lengths between 250 to 400 nm for synthesis time of 8 hours.

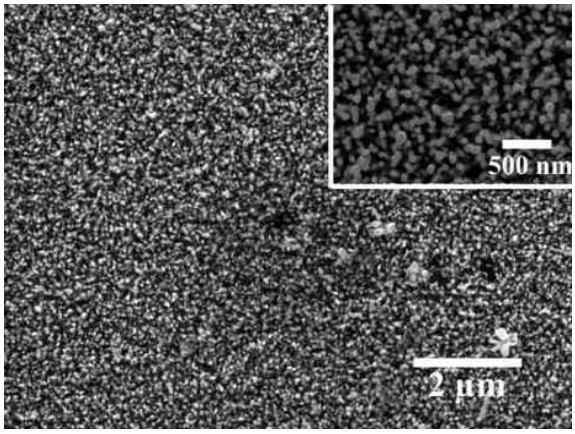

Figure 3: FESEM image of ZnO nanorods in lower magnification surface view, (inset) higher magnification surface view at 90 °C.

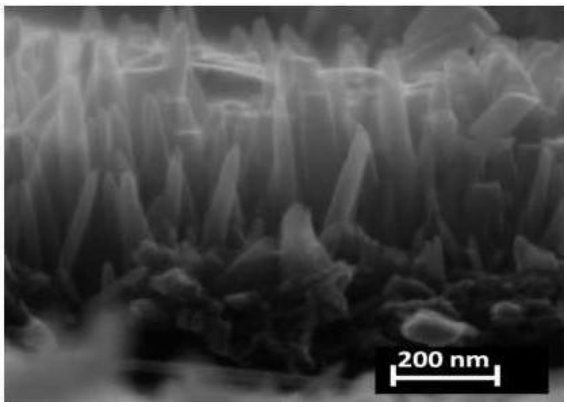

Figure 4: Cross sectional view at 90 °C of ZnO nanorods for synthesis time 4 hours.

The results of this study indicate that there is a threshold temperature for nanorod development at which nanorod formation occurs, and also synthesis time affect nucleation

and subsequent nanorod formation. Considering all the above observations in our experiments, the best growth condition was found to be for a temperature of 90 °C and synthesis time of 8 hours.

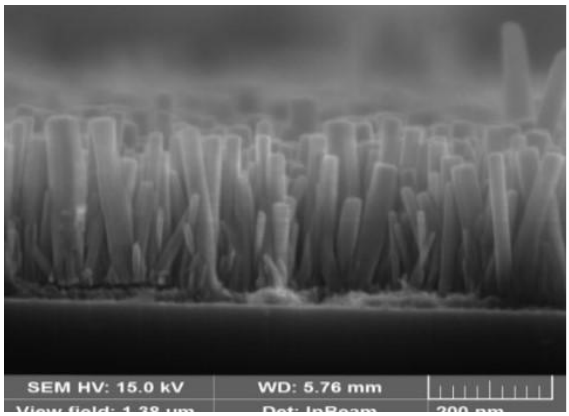

Figure 5: Cross sectional view at 90 °C of ZnO nanorods for synthesis time 8 hours.

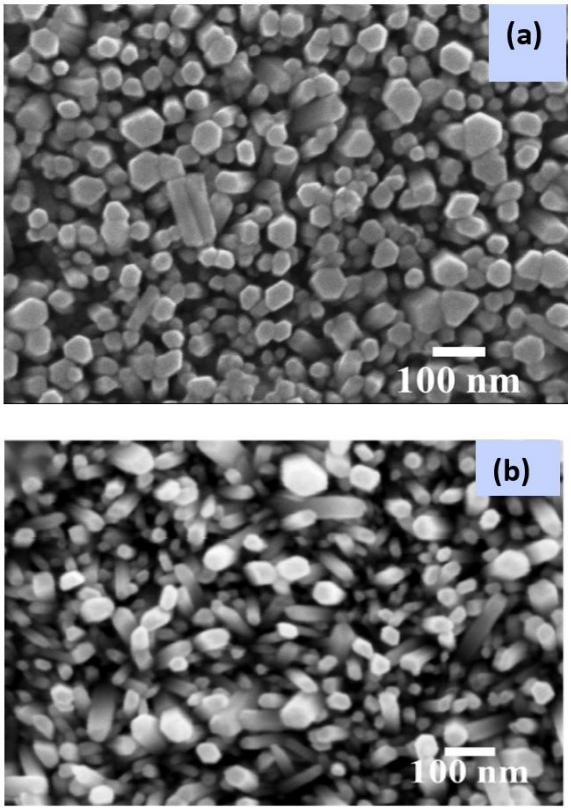

Figure 6: FESEM image of ZnO nanorods grown at different external pressures (a) 0 bar (b) 5 bar.

We have examined the impact of pressure on the growth solution during the hydrothermal synthesis of ZnO nanorods in an autoclave lined with Teflon. A decrease in the length of ZnO nanorods deposited on Zinc foils by a different method with increase in pressure has been reported earlier [39]. The FESEM images of the grown nanorods with varying pressure are shown in Figure 6 (a and b). The nanorods dimensions were measured after synthesis at each pressure. The diameter of the nanorods decreased with increased growth pressure till 5 bar and no significant change in the length was observed. We attribute the declining pattern in the diameter of nanorods to the faster diffusion of reactants from the hydrothermal solution to the surface of the seed layer on the application of pressure, leading to faster collision and hence, oriented attachment of nanoparticles. This prevents the lateral growth of the nanoparticles and hence a decrease in the diameter.

We want to mention here that the nanoparticles sizes in the seed layer affect the sizes of the subsequently grown nanorods. But, by the use of pressure, this constraint is overcome, that is, fine diameter nanorods could be obtained without reducing the seed size or size of nanoparticles in the reacting solution.

Conclusion

Hydrothermal growth of dense and vertically aligned ZnO nanorods on n-type Si substrate with controlled dimensions was demonstrated. The seed layer deposition was optimized with significant improvement in the film quality. The best condition for the growth of nanorods was determined to be for a temperature of 90 °C for 8 hours using 2 mM precursor concentration. The effect of vertical pressure was also explored on the dimensions of the nanorods during the hydrothermal growth. The nanorods diameter was found to be decreasing with increasing pressure. Accordingly, nanorods with the required diameter can be obtained by the application of the appropriate amount of pressure without having to change the underlying seed layer on the substrate. These ZnO nanorods will be further used for fabrication of Piezoelectric Nanogenerator.

Acknowledgement

The authors are thankful to Prof. Joseph Daniel, Principal of Christ Church College, Kanpur for the academic assistance. The authors are also thankful to central instrumentation facility of BIT Mesra, Ranchi for characterization of samples.

References

1. P K Aspoukeh, A A Barzinjy and S M Hamad. Int. Nano Lett., 12(2): 153–168, 2022.
2. Z Tang, J Zhang and Y. Zhang. Adv. Funct. Mater., 32(11): 2113192, 2022.
3. F Qiao, K Sun, H Chu, J Wang, Y Xie, L Chen and T Yan. Battery Energy, 1(1): 20210008, 2022.
4. Md. A Rahman, S M N Mamun, A K M A Hossain and C Ton-That**.** ACS Appl. Nano Mater., 6(17): 15757–15763, 2023.
5. L. Chu, C. Xu, W. Zeng, C. Nie and Y. Hu. IEEE Sens. J., 22(8): 7451–7462, 2022.

6. P G Ramos, L A Sánchez and J M Rodriguez. J Sol-Gel Sci Technol, 102(1):105–124, 2022.
7. M Saeed et al. Chem. Rec., Chem. Rec., 24(1): e202300106, 2023.
8. H Rai and N J M T P Kondal. Mater. Today Proc., 48: 1320–1324, 2022.
9. I Ayoub, V Kumar, R Abolhassani, R Sehgal, V Sharma, R Sehgal, H C Swart and Y K Mishra. Nanotechnol. Rev., 11(1): 575–619, 2022.
10. R Rasmidi, M Duinong and F P Chee. Radiat. Phys. Chem., 184: 109455, 2021.
11. C V Manzano, L Philippe and A Serrà. Crit. Rev. Solid State Mater. Sci., 47(5): 772–805, 2022.
12. M S Krishna, S Singh, M Batool, H M Fahmy, K Seku, A E Shalan, S Lanceros-Mendez and M N Zafar. Mater. Adv., 4(2): 320–354, 2023.
13. B Clarke and K J S Ghandi. Small, 19(44): 2302864, 2023.
14. A F Abdulrahman and N M Abd-Alghafour, Solid-State Electron., 189: 108225, 2022.
15. Q C Bui, G Ardila, H Roussel, C Jiménez, I Gélard, O Chaix-Pluchery , X Mescot, S Boubenia , B Salem and V Consonni. Mater. Adv., 3(1): 498–513, 2022.
16. G Wisz, P Sawicka-Chudy,A Wal, P Potera, M Bester, D Płoch, M Sibiński, M Cholewa and M Ruszała. Appl. Mater. Today, 29: 101673, 2022.
17. J A Mathew, V Tsiumra, J M Sajkowski, A Wierzbicka, R Jakiela, Y Zhydachevskyy, E Przezdziecka, M Stachowicz, A KozaneckiJ. J. Lumin., 251: 119167, 2022.
18. A Al-Rasheedi et al. *Appl. Phys. A.*, 128(9): 782, 2022.
19. P B More, S B Bansode, M Aleksandrova, S R Jadkar and H M Pathan. ES Energy Environ., 22: 983, 2023.
20. C V Manzano, L Philippe and A Serra. Critical Reviews in Solid State and Materials Sciences, 47(5): 772-805, 2021.
21. S Lee, B K Roy and J Cho. Jap. J Appl Phy., 52(5S1): 05DA0952, 2013.
22. Z Zheng, Z S Lim, Y Peng, L You, L Chen, and J Wang. Sci. Rep., 3: 2434, 2013.
23. K H Kim, K Utashiro, Y Abe and M Kawamura. Int J Electrochem Sci., 9: 2080-9, 2014.
24. S López-Romero, P Santiago and D Mendoza. Advanced Science Letters, 10:133-7, 2012.
25. M Bakry, W Ismail, M Abdelfatah and Abdelhamid El-Shaer. Sci Rep 14(1): 23788 (2024).
26. A McLaren, T Valdes-Solis, G Li and S C Tsang. J Am Chem Soc., 131:12540-1, 2009.
27. L Liao, H B Lu, J C Li, H He, D F Wang, D J Fu, C Liu and W F Zhang. *J. Phys. Chem. C*, 111(5): 1900-3, 2007.
28. J Song and S Lim. *J. Phys. Chem. C*, 111(2): 596-600, 2007.
29. Y Tao, M Fu, A Zhao, D He and Y Wang Y. J. Alloys Compd. 489: 99-102, 2010.
30. M Teng, G Min, Z Mei, Z Yanjun and W Xidong. Nanotechnology, 18: 035605, 2007.
31. J J Dong, C Y Zhen, H Y Hao, J Xing, Z L Zhang, Z Y Zheng and X W Zhang. Nanoscale Res Lett, 8: 378 2013.
32. Y Ma, W L Wang, K J Liao and C Y Kong. Journal of Wide Bandgap Materials, 10: 113-20, 2002.
33. A C Dodd, A J McKinley, M Saunders and T Suzuki. J Nanopart Res, 8: 43-51, 2006.
34. L Armelao, M Fabrizio, S Gialanella and F Zordan. Thin Solid Films, 394(1-2): 89-95, 2001.
35. Y Ohya, H Saiki and Y Takahashi. JOURNAL OF MATERIALS SCIENCE, 29: 4099-103, 1994.
36. C Pacholski, A Kornowski and H Weller. Angew Chem Int Ed Engl. 41(7): 1188-91, 2002.
37. H Ghayour, H R Rezaie, S Mirdamadi and A A Nourbakhsh. Vacuum, 86: 101-5, 2011.
38. R M Ziff, E D McGrady and P Meakin. The Journal of Chemical Physics, 82: 5269-74, 1985.
39. L Z Pei, H S Zhao, W Tan, H Y Yu, Y W Chen, C G Fan and Q-F Zhang. Physica E: Low-dimensional Systems and Nanostructures, 42: 1333-7, 2010.